Geophys. J. Int. (2000) **143,** 608–620

Generation of overpressure by cementation of pore space in sedimentary rocks

Magnus Wangen

Institute for Energy Technology, Box 40 N-2007 *Kjeller, Norway. E-mail: magnus@ife.no*

Accepted 2000 May 28. Received 2000 May 8; in original form 1999 November 4

SUMMARY

Overpressure build-up is studied when the main cause for porosity reduction is cementation of the pore space sourced locally. The average porosity reduction for siliclastic sediments is modelled with *n*th-order kinetics. It is shown that the overpressure in one layer at a constant depth will decrease exponentially with time in the case of first-order kinetics for the porosity reduction. The overpressure is studied in one layer subjected to cementation during constant burial along a thermal gradient. A small overpressure build-up is shown above the window for cementation, with a steep rise in overpressure in the upper part of the window. The overpressure build-up is then seen to decrease rapidly towards the end of the window for cementation. Overpressure build-up is also studied when cementation is the main cause for porosity reduction in the entire column of sediments during deposition and burial. The overpressure regime characterized by gravity numbers larger than one is studied. This regime corresponds to low or moderate overpressures in the case of mechanical compaction. Cementation is shown to imply a steep pressure build-up in the window of cementation, which will easily exceed the lithostatic pressure. The porosity loss due to cementation is seen to have a strong impact on the permeability, which leads to the formation of a pressure seal. Although most of the potential for fluid expulsion is exhausted below the seal, because most of the porosity is cemented up, the permeability of the seal is sufficiently low for hydrofracturing to take place. This scenario is consistent with overpressure observations in many wells.

Key words: cementation, overpressure, permeability, porosity.

1 INTRODUCTION

Cementation of the pore space leads to expulsion of the pore fluid. The cementation process consists of the precipitation of minerals in the pore space, with the minerals then displacing the pore fluid. Furthermore, the permeability is reduced when porosity is lost. Cementation processes are therefore believed to be an important cause for pressure build-up in sedimentary basins because they imply both the expulsion of fluid and the formation of seals (Bjørkum & Nadeau 1996, 1998; Osborn & Swarbrick 1997; Hunt 1990; Powley 1990).

Pressure–depth trends often show a transition from hydrostatic fluid pressure to almost lithostatic fluid pressure over a depth interval that is less than 1.5 km (Leonard 1993; Gaarenstrom 1993; Darby *et al.* 1996; Bjørkum & Nadeau 1998). The characteristics of the fluid pressure and the transition zone are shown in Fig. 1. The pressure is close to the hydrostatic pressure above the transition zone, it rises steeply towards the lithostatic pressure in the transition zone, and it follows a gradient which is close to the hydrostatic pressure gradient below the transition zone. Fig. 1 also shows the characteristics of the pressure transition zone as overpressure, which is the fluid pressure minus the hydrostatic pressure. The overpressure is therefore bounded by zero and the lithostatic pressure minus the hydrostatic pressure, where the later pressure is called the excess lithostatic pressure. (See Appendix A for a precise definition of the excess lithostatic pressure.) The aim of this paper is to explore cementation of the pore space as a possible explanation for the development of pressure transition zones.

Overpressure build-up has traditionally been modelled using porosity as a function of effective vertical stress, an approach that has been successful in soil mechanics. This kind of porosity reduction is called mechanical compaction, and it has been shown by several authors to model overpressure build-up during the rapid burial of low-permeability sediments (Gibson 1958; Bredehoeft & Hanshaw 1968; Smith 1971; Sharp 1976; Sharp & Domenico 1976; Bethke & Corbet 1988; Lerche 1990; Luo & Vasseur 1992; Audet & Fowler 1992; Wangen 1992, 1997). Compaction computed as a function of effective stress is appropriate for the youngest and uppermost sediments. However, it is not clear how well suited this concept is for lithified (cemented) rocks at a greater depth. Some authors argue that

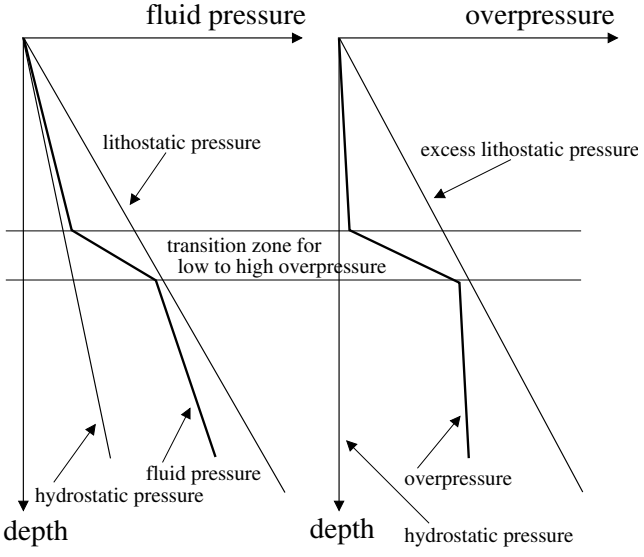

Figure 1. A pressure transition zone is shown as fluid pressure to the left and overpressure to the right. The overpressure is the fluid pressure in excess of the hydrostatic pressure. The fluid pressure is close to the hydrostatic pressure above the transition zone, it rises towards the lithostatic pressure in the transition zone, and it follows a pressure gradient that is close to the hydrostatic pressure below the zone. Note that a fluid pressure gradient that is parallel to the hydrostatic pressure corresponds to an overpressure gradient that is vertical.

chemical processes are more important for the porosity loss when the sediments become lithified (Dewers & Ortoleva 1990; Oelkers *et al.* 1996; Bjørlykke & Høeg 1997; Bjørkum & Nadeau 1998; Bjørlykke 1999a,b), and that the process is less controlled by pressure (or effective stress) than temperature.

Several alternatives to mechanical compaction have been studied. One simple approach is to model overpressure build-up during burial when the porosity is assumed known as a function of depth (Wangen 1997). The exponentially decreasing porosity with depth observed by Athy (1930) is an example of such a porosity–depth function. Another alternative that has been studied is the compaction of sediments assuming viscoelastic/viscoplastic behaviour (Birchwood & Turcotte 1994; Schneider 1996; Fowler & Yang 1999).

The possibilities for the cementation of pore space to cause a build-up of pressure are studied here with simple models. A major challenge with such modelling is the cementation part. Mineral dissolution and reprecipitation in the pore space are very complex processes, with many poorly understood aspects. Such processes are therefore difficult to model (Lichtner 1985, 1988). The minerals dissolved in one place can be transported with the fluid to other places, where they are precipitated. This is typical for most common minerals acting as a cement, for instance carbonates, which can be sourced both locally and distantly. A general approach to cementation modelling would therefore need to couple the mineral transport to the fluid flow. Instead of attempting to model all aspects of the cementation process, we restrict ourselves to cement sourced locally, which is a reasonable assumption for at least quartz cement (Bjørkum 1994, 1996). We simply assume that the cementation process can be modelled as an *n*th-order Arrhenius law for the rate of change of porosity. This model was suggested for quartz cementation sourced locally by Wangen (1999).

Three simple models are studied where pressure build-up is caused by the cementation of the pore space. The first model considers fluid expulsion and pressure build-up in a sandstone layer at a given depth. The second model does the same for a sandstone layer during burial. The third model goes further and considers cementation as the main cause of pressure build-up in an entire sedimentary column during burial. This model is based on an 'average' lithology, where the cementation process is still assumed to be an *n*th-order Arrhenius law. The cementation model originally suggested for sandstones is then extrapolated to a model representing an ensemble of sediments including sandstones, siltstones and shales. It is possible to include shales in such an average because shales will normally lose most of their porosity at shallow depths due to mechanical compaction. Shales are therefore assumed to be less important fluid reservoirs than sandstones. Hermanrud *et al.* (1998) did not observe any relationship between overpressure and porosity in shales in the Norwegian Continental Shelf at temperatures greater than 110 °C. They suggested that thermally controlled mineral reactions were responsible for the porosity reduction at temperatures greater than 100 °C. This diagenetic effect is considered to be accounted for in the model for porosity reduction. The Arrhenius parameters are therefore assumed to represent an average lithology, rather than a sandstone. Shales are important for the average permeability of an ensemble of lithologies. Shales are accounted for by the permeability function, which relates diagenetically altered porosity to permeability. Shales will also have their permeabilities strongly reduced by diagenetic illite formation at temperatures as high as 150 °C (Bjørkum & Nadeau 1998). This type of diagenetic process in shales is not a part of the model. Although the third model is at best a crude description of the pressure build-up caused by diagenetic alterations of the sediments, it nevertheless captures the transitional zone for low to high overpressure. This is an essential feature of fluid pressures in many sedimentary basins (Bjørkum & Nadeau 1998).

The use of one lithology to represent an ensemble of lithologies is quite common because it allows for analytical considerations. Examples of such models are those of Gibson (1958), Bredehoeft & Hanshaw (1968), Smith (1971), Sharp (1976), Sharp & Domenico (1976), Bethke & Corbet (1988), Lerche (1990), Luo & Vasseur (1992), Audet & Fowler (1992), Lamée & Guéguen (1996), Wangen (1992, 1997) and Fowler & Yang (1998, 1999).

This paper is organized as follows. The gravity numbers characterizing overpressure regimes and the cementation model are reviewed first. The overpressure build-up due to the cementation of a single layer kept at a constant depth is investigated, and then the same is done for a layer during constant burial along a constant thermal gradient. The fluid expulsion rates out of a layer during burial are then estimated. Finally, the overpressure build-up due to cementation of an entire 1-D column is calculated during burial.

2 CHARACTERIZATION OF OVERPRESSURE BUILD-UP BY THE GRAVITY NUMBER

The overpressure build-up in sedimentary basins can be characterized by the (dimensionless) gravity number,

$$N_g = \frac{\bar{k}(\rho_s - \rho_f)g}{\mu\omega}, \qquad (1)$$

where $\bar{k}$ is the average permeability of the sediments, μ is the viscosity, ω is the burial rate, and ρ_s and ρ_f are the density of the sediment matrix and the fluid, respectively. A gravity number $N_g = 1$ was shown by Audet & Fowler (1992) and Wangen (1992) to define a transitional regime between low and high overpressures. The regime $N_g \gg 1$ yields low overpressures, which means that the fluid pressures are close to the hydrostatic pressure. The regime $N_g \ll 1$ yields high overpressures, which corresponds to fluid pressures close to the lithostatic pressure. The gravity number can be interpreted in terms of a maximal Darcy velocity during burial relative to the burial rate. The maximal Darcy velocity, obtained when the fluid pressure is equal to the lithostatic pressure, is approximately $v_{max} = (\bar{k}/\mu)(\rho_s - \rho_f)g$. High overpressure, given by the regime $N_g \ll 1$, is then seen to be the same as $v_{max}/\omega \ll 1$. High overpressure develops when the Darcy velocity given by a fluid pressure gradient parallel to the lithostatic pressure gradient is insufficient to keep pace with the burial rate. On the other hand, if the lithostatic pressure gradient yields Darcy velocities that are much larger than the burial rate, then a low pressure gradient is sufficient to provide a Darcy velocity that can keep pace with the burial rate.

Wangen (1997) showed that the pressure build-up could easily reach far beyond the lithostatic pressure during burial for $N_g \ll 1$ when the porosity was given as a function of depth. This regime therefore leads to hydrofracturing. It was suggested in Wangen (1997) that the average permeability of hydrofractured sedimentary rocks during burial corresponds to $N_g = 1$.

3 POROSITY EVOLUTION CAUSED BY CEMENTATION

The rate of change of porosity can be written as

$$\frac{d\phi}{dt} = -k_f(T)S(\phi)v_q c \tag{2}$$

when precipitation is controlled by the degree of supersaturation,

$$c = \frac{(m - m^{eq})}{m^{eq}}, \tag{3}$$

for one mineral cement species, for instance quartz. The concentration of the mineral cement in the pore fluid is m and the equilibrium concentration is denoted m^{eq}. The coefficient k_f (mol m^{-2} s^{-1}) is the forward reaction rate of the mineral cement, $S(\phi)$ is the porosity-dependent specific surface area for precipitation (m^2 m^{-3}), and v_q (m^3 mol^{-1}) is the molar volume of the mineral cement. The rate $k_f(T)$ is given by an Arrhenius law,

$$k_f = A_f \exp\left(-\frac{E_f}{RT}\right), \tag{4}$$

where A_f (mol m^{-2} s^{-1}) is the Arrhenius prefactor and E_f (kJ mol^{-1} K^{-1}) is the activation energy. The temperature T is given in Kelvins. The specific surface as a function of porosity is assumed to be a simple power law in the porosity,

$$S(\phi) = S_0\hat{S}(\phi), \quad \text{where} \quad \hat{S}(\phi) = \left(\frac{\phi - \phi_c}{\phi_0 - \phi_c}\right)^n, \tag{5}$$

and where the exponent n must be fitted to a particular porous medium. The parameter S_0 (m^2 m^{-3}) is the specific surface at the initial porosity ϕ_0, and ϕ_c is a lower boundary for porosity reduction, where the pore space of the medium becomes disconnected. The specific surface of the medium becomes zero when the pores become disconnected. This porosity function implies that the expression for the rate of change of porosity becomes an nth-order Arrhenius law, given that the degree of supersaturation can be assumed either constant or given in the form of an Arrhenius law. For the latter case, where the degree of supersaturation is given in the form of an Arrhenius law, the product of the two Arrhenius laws (the supersaturation and the reaction rate) can be rewritten as a constant degree of supersaturation times one Arrhenius law for the reaction rate (Wangen 1999). The new reaction rate then has modified Arrhenius parameters accounting for the Arrhenius behaviour of the degree of supersaturation. It should be noted that no cementation will occur unless there is supersaturation.

The expression (2) for the rate of change of porosity has been used to model quartz cementation of sandstones, when silica is sourced locally from stylolites or other quartz–mica contacts. There is strong petrographic evidence for mica being a catalyst for the dissolution of quartz (Oelkers *et al.* 1992, 1993, 1996; Bjørkum 1994, 1996; Walderhaug 1994a,b, 1996; Aase *et al.* 1996). This work also shows that the precipitation step is the slowest step in the process. Dissolution of silica at stylolites or at other quartz–mica contacts therefore maintains a supersaturation of silica that is almost uniform locally, as long as diffusion can keep pace with precipitation. Petrographic work has estimated the degree of supersaturation to be ~ 0.01 in the temperature window where quartz cementation operates (Aase *et al.* 1996). Porosity predictions based on this model have been made by Oelkers *et al.* (1996), Walderhaug (1996), Bjørkum *et al.* (1998) and Wangen (1998, 1999). Oelkers *et al.* (1996) solved the diffusion–reaction equation for the silica supersaturation between the stylolites numerically in order to obtain the precipitation rates of quartz. Bjørkum *et al.* (1998) extended this model to porosity predictions in the presence of hydrocarbons, and compared the porosity predictions to a set of observation. Walderhaug (1996) computed porosity reduction in sandstone reservoirs based on an empirical expression for the quartz precipitation rate as a function of temperature (Walderhaug 1994a).

Wangen (1998, 1999) suggested analytical expressions for the porosity evolution as a function of time and temperature in the isothermal case and the case of a piecewise linear burial history. These expressions are based on expression (2) for the rate of change of porosity, which becomes an nth-order Arrhenius law when the specific surface is given by the function (5). Eq. (2) is straightforward to integrate in the isothermal case, and the porosity as a function of temperature and time is (Wangen 1999)

$$\phi(t) = \begin{cases} \phi_c + (\phi_0 - \phi_c)\left(1 - \dfrac{(1-n)}{\phi_0}\, c\, v_q S_0 k_f(T) t\right)^{1/(1-n)}, & n \neq 1, \\ \phi_c + (\phi_0 - \phi_c)\exp\left(-\dfrac{1}{\phi_0}\, c\, v_q S_0 k_f(T) t\right), & n = 1, \end{cases} \tag{6}$$

where ϕ_c is the porosity at the percolation threshold. The pore connectivity becomes zero at non-zero porosity in the region of 3–5 per cent. Reduction of the porosity below the critical porosity ϕ_c is therefore impossible, even though the cementation process operates locally to just a few grains. The nth-order

Arrhenius equation is difficult to integrate exactly in the case of burial at a constant rate along a constant thermal gradient dT/dz,

$$T = T_0 + \frac{dT}{dz}\,\omega t\,, \tag{7}$$

where T_0 is the surface temperature and ω is the burial rate. However, there are good approximations, for example, that of Wangen (1999):

$$\phi(T) = \begin{cases} \phi_c + (\phi_0 - \phi_c)\{1-(1-n)N_B(F(T)-F(T_0))\}^{1/(1-n)}\,, \\ \qquad\qquad\qquad\qquad\qquad\qquad n \neq 1\,, \\ \phi_c + (\phi_0 - \phi_c)\exp\{-N_B(F(T)-F(T_0))\}\,, \quad n = 1\,, \end{cases} \tag{8}$$

where $F(T)$ is the function

$$F(T) = (T/T_f)^2 \exp(-T_f/T)\,, \tag{9}$$

with $T_f = E_f/R$ and where the number N_B is

$$N_B = \frac{c\,v_q S_0 A_f E_f}{\phi_0 R \omega\,(dT/dz)}\,. \tag{10}$$

The exponent n in function (5) controls how fast the specific surface approaches zero. Different regimes exists depending on whether $n<1$ or $n\geq 1$, and it is seen that for $n<1$ the porosity will reach ϕ_c within a finite time or within a finite temperature range during burial. On the other hand, when $n\geq 1$, ϕ will then approach ϕ_c asymptotically with time and temperature during burial (Wangen 1999).

The two expressions (6) and (8) for the porosity reduction caused by cementation as a function of time and temperature apply for a pore space of well-sorted grains. In particular, the initial porosity and the initial specific surface will vary greatly over short distances, as seen from well logs. The expressions (6) and (8) must be averaged over an ensemble of different grain sizes in order to represent tens of metres of sedimentary rocks. The temperature of an interval of sedimentary rocks can be considered uniform as long as the temperature difference between the top and the bottom of the interval is less than ~ 1 °C. An ensemble average for the porosity in the interval can then be obtained in a direct manner,

$$\bar{\phi}(T) = \sum_i w_i \phi_i(T)\,, \tag{11}$$

where w_i is the fraction of each porosity sample ϕ_i in the ensemble. (A bar above a symbol denotes an average quantity.) An alternative to the weighted mean, given by the porosity function (11), is to fit the activation energy and the initial specific surface for one single porosity function to obtain a best match to the porosity evolution of the ensemble.

A reduction in porosity also leads to a reduction in permeability. The average permeability of the ensemble is not easily expressed by the average porosity, because some samples in the ensemble will lose their porosity much earlier than other samples, which can have a strong effect on the average permeability. The average vertical permeability will be strongly reduced in an interval if a thin subinterval therein becomes completely cemented, while the average porosity of the interval may be only slightly reduced.

The pressure build-up caused by cementation is found to be strongly connected to the sealing effect of porosity approaching the percolation threshold ϕ_c. However, it is uncertain how well the porosity predictions given by eqs (6) and (8) represent the porosity reduction that takes place close to the percolation threshold (Sahimi 1994).

The use of averaged porosity functions is unavoidable when dealing with overpressure modelling on a basin scale, because of the large size of the system. Sedimentary rocks are so heterogeneous that they are very difficult to model, except when their properties are represented by averages.

4 OVERPRESSURE WITHOUT BURIAL

The first and simplest situation to be considered is the expulsion of fluid from a layer undergoing cementation in a basin during a pause in sedimentation. The layer is at a depth z and the overlying sediments have an average permeability $\bar{k}$. The vertical Darcy velocity (volume flux) out of the layer in a 1-D column is then

$$v_{cem} = -h\,\frac{\partial \phi}{\partial t}\,, \tag{12}$$

where h is the thickness of the layer undergoing cementation. This Darcy velocity can be expressed by means of the average permeability and the overpressure gradient p/z, where p is the overpressure in the layer. The overpressure p is then

$$p = -\frac{\mu z h}{\bar{k}}\,\frac{\partial \phi}{\partial t}\,, \tag{13}$$

where μ is the viscosity of water. The expression for $\partial\phi/\partial t$ is given by eq. (2) and the isothermal porosity evolution is given by eq. (6). The overpressure p can therefore be written as

$$p = p_0 \exp(-t/t_0) \tag{14}$$

for $n=1$ (first-order kinetics), where

$$p_0 = \frac{\phi_0 \mu z h}{t_0 \bar{k}} \quad \text{and} \quad t_0 = \frac{\phi_0}{c\,v_q S_0 k_f(T)}\,. \tag{15}$$

The initial porosity ϕ_0 here is the porosity at $t=0$ in the reservoir layer. It is seen from expression (14) that the maximum overpressure is given by p_0 at $t=0$, and that the overpressure then decays exponentially with a half-life $t_{1/2} = t_0 \log(2)$. In order to evaluate the pressure, it is instructive to compare it to the lithostatic pressure. Recall that the overpressure is the pore fluid pressure minus the hydrostatic pressure; the overpressure will therefore be compared with the lithostatic pressure minus the hydrostatic pressure, which is termed the excess lithostatic pressure. The excess lithostatic pressure, denoted σ', can be written as $\sigma' = \Delta\rho g(1-\bar{\phi})z$, where $\Delta\rho = \rho_s - \rho_f$ is the density difference between the sediment grains and the fluid, and $\bar{\phi}$ is the average porosity down to the depth z. See Appendix A for details of how the excess lithostatic pressure is calculated. The overpressure coefficient p_0, measured relative to the excess lithostatic pressure, is then

$$\hat{p}_0 = \frac{\phi_0 \mu h}{t_0 \bar{k} \Delta\rho g (1-\bar{\phi})}\,, \tag{16}$$

where a hat above a symbol denotes a dimensionless quantity. Notice that the depth, z, to the reservoir layer drops out of the dimensionless pressure $\hat{p}_0$. The fluid pressure is initially at the lithostatic pressure when $\hat{p}_0 = 1$. The condition for pressures

bounded above by the lithostatic pressure is given as

$$\frac{\bar{k}\Delta\rho g}{\phi_0\mu(h/t_0)}(1-\bar{\phi}) > 1\,. \tag{17}$$

An equality in condition (17) implies pressures at the lithostatic level. The form of the gravity number is recognized in condition (17) for high overpressures, where h/t_0 replaces the burial rate. The time constant t_0 needs to be calculated before condition (17) can be used to estimate an upper bound on the permeability $\bar{k}$. This time constant is dependent on the temperature because of the reaction rate $k_f(T)$. This is seen in Fig. 2, where t_0 is plotted as a function of temperature, based on the data in Table 1. The time constant t_0 changes by more than four orders of magnitude from 0 to 100 °C. At 100 °C, the time constant is ~1 Myr. The direct implication of the temperature dependence in t_0 is that overpressures generated by cementation decay much faster than 1 Myr at depths with temperatures larger than 125 °C.

It is seen from eq. (17) that p_0 reaches the lithostatic pressure for $t_0 = 1$ Myr when $\bar{k} = 1\times10^{-19}$ m^2. The other parameters in eq. (17) are as follows: $h = 70$ m, $\bar{\phi} = 0.3$, $\mu = 1\times10^{-3}$ Pa s, $\Delta\rho g = 1\times10^{4}$ Pa m^{-1} and $\phi_0 = 0.315$.

It is seen from eq. (15) that p_0 is inversely proportional to t_0, and that the pressure decays exponentially on a timescale t_0. A 'short' t_0 therefore implies a 'high' overpressure lasting a 'short' time, while a 'long' t_0 implies a 'low' overpressure lasting a 'long' time.

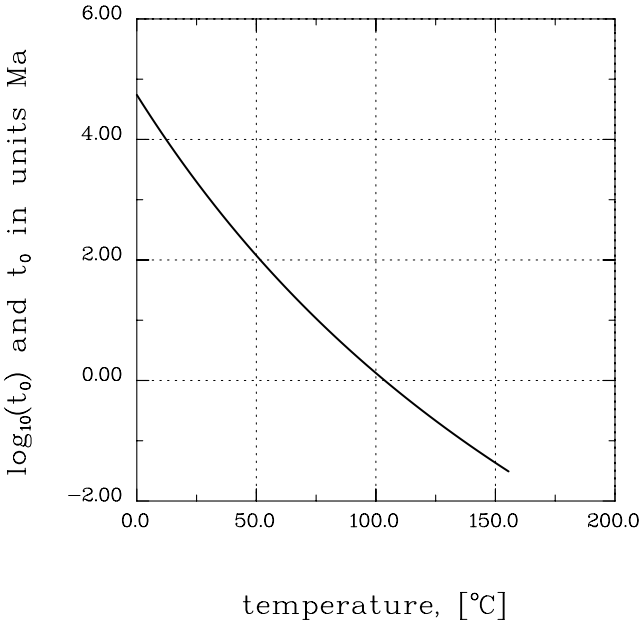

Figure 2. The characteristic time t_0 for isothermal cementation is plotted as a function of temperature.

5 OVERPRESSURE IN A LAYER DURING BURIAL

The model in the preceding section can be refined by considering a layer during burial. The depth down to the layer is now a linear function of time, $z = \omega t$. The temperature also increases linearly with time because the temperature gradient is assumed constant (see eq. 7). An expression for the overpressure, based on eq. (13), can be written as

$$p(T) = \frac{\mu\omega t h}{\bar{k}}\, c\, v_q k_f(T) S(\phi(T))\,, \tag{18}$$

where T is used instead of time. Note that time, temperature and depth are all linearly related (see eq. 7). The porosity as a function of temperature during constant burial is given

Table 1. The parameter set. The data for quartz kinetics are taken from Tester *et al.* (1994) (see Wangen 1998). Bjørkum *et al.* (1998) used a specific surface area function $S(\phi)\sim(\phi-0.035)$, which corresponds to $n=1$. The degree of supersaturation c is taken from Aase *et al.* (1996). The diffusion coefficient of aqueous silica in pure solution is based on data from the CRC handbook (Weast 1976).

Symbol	Value	Units	Comment
A_f	24	mol m^{-2} s^{-1}	Arrhenius factor
E_f	90	kJ mol^{-1} K^{-1}	Activation energy
R	8.314	mol kg^{-1} s^{-1}	Gas constant
c	0.01	–	Degree of silica supersaturation
S_0	5×10^3	m^2 m^{-3}	Initial specific surface
n	1	–	Specific surface exponent
v_q	$2.4\times\ 10^{-5}$	m^3 mol^{-1}	Molar volume of quartz
ω	50	m Myr^{-1}	Burial rate
ϕ_0	0.3	–	Initial porosity
$T_f = E_f/R$	10 825	K	
dT/dz	0.03	°C m^{-1}	Thermal gradient
a	900.7	–	Parameter in approximation of F
b	−66.9	–	Parameter in approximation of F
k_0	1×10^{-18}	m^2	Permeability at $\phi=\phi_0$
μ	1×10^{-3}	Pa s	Viscosity
ρ_f	1000.0	kg m^{-3}	Fluid density
ρ_s	2000.0	kg m^{-3}	Sediment matrix density
ϕ_c	0.05	–	Critical porosity
m	3	–	Permeability exponent
n	1	–	Specific surface exponent

by function (8), and it is inserted into the function for the specific surface, which is a function of the porosity. The specific surface as a linear function of porosity is considered ($n=1$). The overpressure p is divided by excess lithostatic pressure, $\sigma'=\Delta\rho g(1-\bar{\phi})\omega t$, for easier evaluation. The overpressure scaled with the excess lithostatic pressure can be written as

$$\hat{p}(T)=\hat{p}_0 f(T)\,, \tag{19}$$

where $\hat{p}_0$ is the constant of proportionality,

$$\hat{p}_0=\frac{\mu h\, c\, v_q S_0 A_f}{\bar{k}\Delta\rho g(1-\bar{\phi})}\,, \tag{20}$$

and where $f(T)$ is the temperature-dependent part of the pressure,

$$f(T)=\exp\left(-\frac{T_f}{T}-N_B(F(T)-F(T_0))\right). \tag{21}$$

The function $f(T)$, which yields the pressure in the layer during burial, is plotted in Fig. 3. From Fig. 3 it is seen that the overpressure increases with depth until some maximum, where it decreases rapidly. The overpressure increases for temperatures less than the maximum because the reaction rate increases while the porosity remains a substantial fraction of ϕ_0. The reaction rate still increases for temperatures above the maximum, but the porosity becomes almost zero and $f(T)$ therefore decreases. In order to evaluate the maximum overpressure, it is necessary to estimate the maximum of $f(T)$. A reasonably good estimate for the maximum is

$$f(T_{max})=\frac{\exp(-1)}{N_B}\left(\frac{T_f}{T_{max}}\right)^2\approx\frac{\exp(-1)a^2}{N_B(\log(N_B)+b)^2}\,, \tag{22}$$

where T_{max} is the temperature where $f(T)$ attains its maximum. This estimate is derived in Appendix B, which also explains parameters a and b. It is also shown in Appendix B that the temperature T_{max} is close to the temperature where the porosity

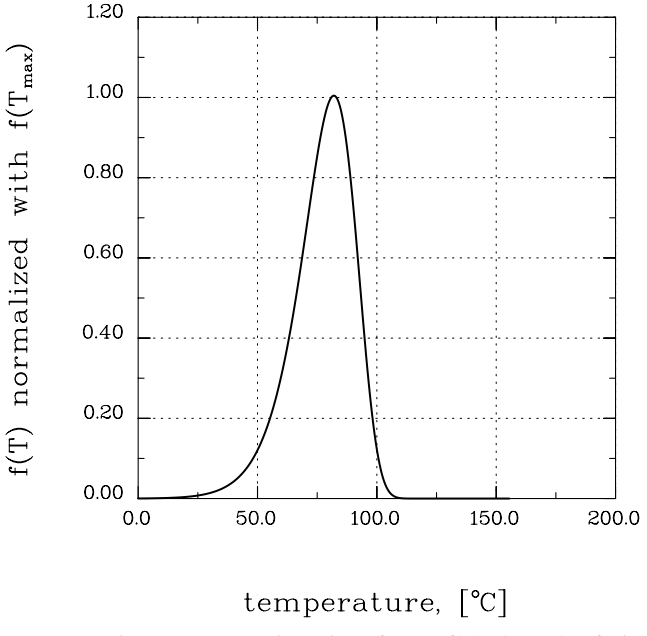

Figure 3. The temperature-dependent factor $f(T)$ (eq. 21) of the pressure in a layer during cementation. The function $f(T)$ is shown normalized by its maximum $f(T_{max})$

has decreased to half its initial value. From eqs (20) and (22), the maximum overpressure relative to the excess lithostatic pressure is then

$$\hat{p}_{max}=\frac{1}{N_g}\frac{\phi_0\exp(-1)}{(1-\bar{\phi})}\frac{T_f\Delta T}{T_{max}^2}\,, \tag{23}$$

where $\hat{p}_0$ is rewritten in terms of the numbers N_g and N_B. The temperature difference across the reservoir, $\Delta T=(dT/dz)h$, is used in place of the reservoir thickness. It is now possible to estimate how likely overpressure is in the layer during burial. If we assume that $T_{max}\sim 100$ °C, $\phi_0\exp(-1)/(1-\bar{\phi})\sim 1.5$ and the thickness of the layer h times the thermal gradient is ~ 8.5 °C, then we have $\hat{p}_{max}\sim 1/N_g$.

The maximum overpressure in the layer is seen to be inversely proportional to N_g. The necessary condition for large overpressures is then $N_g\ll 1$, and the overpressures will correspond to fluid pressures close to the hydrostatic pressure for $N_g\gg 1$. The gravity number is therefore a useful parameter for the characterization of pressure build-up in a layer undergoing cementation.

6 FLUID EXPULSION RATES

The model for overpressure build-up in the previous section did not consider other sources for fluid than what is expelled from one reservoir layer during cementation. The overpressure build-up could be larger if the reservoir layer drains fluids expelled from layers below. The amount of fluid expelled from the reservoir during burial is therefore compared with what could be expelled from the sedimentary rocks below. The latter fluid flux is estimated by assuming that the porosity below the layer is known as a function of depth. The Darcy velocity in the vertical direction is then (see Appendix C)

$$v=\omega(e-e_{bot})\,. \tag{24}$$

The Darcy velocity out of a column of sediments during burial, at the position where the void ratio is e, is seen to be proportional to the burial rate and the difference between e and the void ratio at the bottom of the column, e_{bot}. The fluid flux out of the layer due to cementation, v_{cem}, is given by eq. (12). This flux can be expressed by means of the function $f(T)$, just like $\hat{p}(T)$ in eq. (19). The flux out of the layer due to cementation relative to flux from below is then

$$\frac{v_{cem}}{v}=N_B\frac{\phi_0}{(e-e_{bot})}\frac{\Delta T}{T_f}f(T)\,, \tag{25}$$

where the temperature difference across the layer is used instead of the layer thickness. The maximum of the ratio v_{cem}/v can be estimated by using expression (22) for the maximum of the function $f(T)$,

$$\left(\frac{v_{cem}}{v}\right)_{max}=\exp(-1)\frac{\phi_0}{(e-e_{bot})}\frac{T_f\Delta T}{T_{max}^2}\,. \tag{26}$$

The temperature T_{max} is given by the estimate (B6). The condition for the amount of fluid expelled from the reservoir layer to be greater than what is expelled from the sediments below is $(v_{cem}/v)_{max}>1$. This condition becomes

$$\Delta T>(e-e_{bot})70\ ^\circ\mathrm{C} \tag{27}$$

when $T_f=10\,825$ K, $T_{max}=95$ °C and $\phi_0=0.5$. Assuming furthermore that $(e-e_{bot})\approx 0.15$, it is seen that $\Delta T>10.5$ °C

for fluid expulsion from the reservoir layer to exceed what is coming from below. This temperature difference across a layer is equivalent to a thickness ~ 300 m when the thermal gradient is 35 °C m^{-1}. Judging from condition (27), it is therefore possible that the cementation of a sandstone sequence a few hundred metres thick could expel an amount of fluid comparable to that expelled from the entire column of sedimentary rocks below.

7 CEMENTATION AS THE MAIN CAUSE OF POROSITY REDUCTION

Another end-member for pressure build-up caused by cementation is the model where cementation is the only cause of porosity reduction in the entire sedimentary column. The first-order Arrhenius kinetics for porosity reduction is considered as an average kinetics, which is calibrated to a wider range of sediments than just quartzose sandstones. The Arrhenius parameters are assumed to represent the average of a variety of grain sizes dominated by siliclastic minerals. The porosity functions (8) will represent the porosity in the entire column of sediments. The porosity description now spans sandstones, siltstones and shales. Shales are assumed to have lost most of their porosity due to mechanical compaction at shallow depths. Therefore, shales contribute less to the expulsion of fluids than sandstones and siltstones at temperatures where cementation starts to operate. However, shales are important with respect to the average permeability of an ensemble of lithologies. The effect of shales on the permeability is accounted for by the permeability function, which yields an average permeability from an average porosity.

Temperature is, as before, used instead of depth because these two quantities are linearly related. Analytical expressions for the overpressure are then possible for burial at a constant rate along a constant thermal gradient.

The calculation of Darcy velocities and overpressures in compacting basins is simplified when carried out in the completely compacted vertical coordinate, here denoted ζ, rather than the real z-coordinate. The ζ-coordinate measures the height of a point in the basin from the basement as porosity-free rock, and it is therefore a Lagrange coordinate. This Lagrange coordinate was previously used to study pressure build-up (Wangen 1992, 1997). See also Appendix A, where the excess lithostatic pressure is calculated using the ζ-coordinate. The ζ height to the top of the basin (the ζ-coordinate of the basin surface) is denoted ζ^*.

The Darcy velocity in the vertical direction is also given by expression (24) when the porosity (or the void ratio) is a function of temperature during constant burial along a constant thermal gradient (see Appendix C). The burial rate is now constant when given as compacted (porosity-free) sediments, and the thermal gradient is constant when measured along the ζ-axis. In other words, both $\partial\zeta^*/\partial t$ and $\partial T/\partial\zeta$ are constant. A constant $\partial T/\partial\zeta$ implies that $\partial T/\partial z$ is not constant, which is seen in Fig. 4, where T is plotted as a function of depth, z. Fig. 4 shows that $\partial T/\partial z$ is close to linear above the window for cementation and below the window for cementation. That is because $\phi \approx \phi_0$ above the window and $\phi \approx \phi_c$ below the window. The computation of overpressure is now based on a constant $\partial T/\partial\zeta$, which implies that $\partial T/\partial z$ in the number N_B (eq. 10) is replaced by $\partial T/\partial\zeta$.

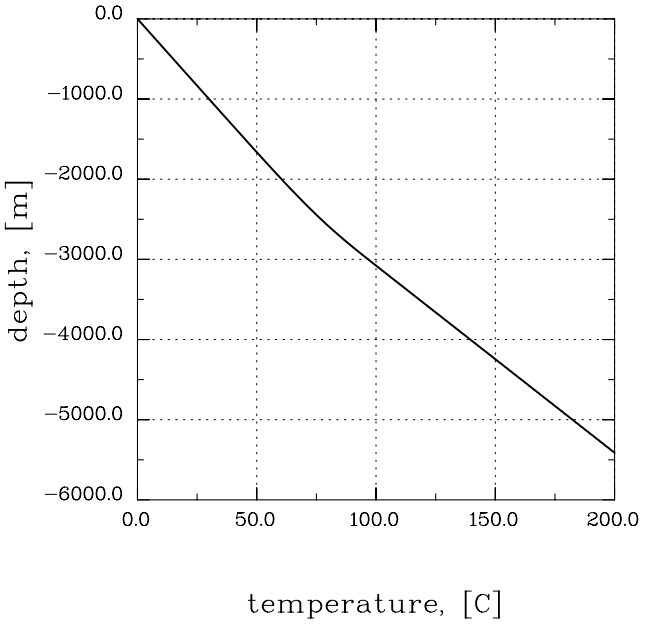

Figure 4. Temperature plotted as a function of depth for $\partial T/\partial\zeta^* = 0.043$ °C m^{-1}. The ζ-coordinate is related to the z-coordinate by eq. (A3). (The porosity used to obtain z from ζ is plotted in Fig. 8 for $n = 1$.)

Darcy's law, expressed along the ζ-axis, combined with expression (24) for the fluid flux at any position in the sedimentary column, then yields

$$\frac{\partial p}{\partial \zeta} = -\frac{(1+e)\mu\omega}{k(\phi)}(e - e_{\mathrm{bot}}), \tag{28}$$

where $k(\phi)$ is a porosity-dependent permeability function. (See Appendix C for a derivation of the fluid flux caused by cementation during burial.) The permeability function is chosen to be

$$k(\phi) = k_0 \frac{(1+e)(1-\phi_0)}{(1+e_0)(1-\phi)}\left(\frac{\phi-\phi_c}{\phi_0-\phi_c}\right)^m, \tag{29}$$

where k_0 is the permeability at initial porosity ϕ_0. This permeability function is basically a Kozeny–Carman type of permeability function because $k(\phi) \sim (\phi - \phi_c)^m$ for small porosities. Note that the permeability approaches zero when ϕ approaches the critical porosity ϕ_c, which is consistent with ϕ_c being the porosity at the percolation threshold. The factors $(1+e)/(1+e_0)$ and $(1-\phi_0)/(1-\phi)$ in the permeability function are numbers close to 1, and they are therefore not important for the permeability. However, these factors are included because they simplify the analytical treatment of the overpressure considerably. Note that initial permeability k_0 and the permeability exponent m are assumed to represent an ensemble of lithologies. Although the Kozeny–Carman equation has normally been used for sands and sandstones, it can also be applied to compacted shales (Ungerer *et al.* 1990). Ungerer *et. al* (1990) used $m = 3$ for sandstones and $m = 5$ for shales, with a much lower initial permeability k_0 for shales than for sandstones. Fowler & Yang (1999) applied a Kozeny–Carman equation with m as high as 8 for low-permeability sediments.

The pressure is obtained by integrating eq. (28) from ζ to ζ^*, after inserting the permeability function, which then yields

$$p = c_0 \int_{\zeta}^{\zeta^*} ((1+e_{\rm bot})(\phi-\phi_{\rm c})^{1-m} + (\phi_{\rm c}-(1-\phi_{\rm c})e_{\rm bot})(\phi-\phi_{\rm c})^{-m})\, d\zeta\,, \tag{30}$$

where the constant c_0 is

$$c_0 = \frac{(1+e_0)(\phi_0-\phi_{\rm c})^m \mu\omega}{(1-\phi_0)k_0}\,. \tag{31}$$

Note that the last term in the integral becomes zero when the basin becomes deep enough for $e_{\rm bot}=\phi_{\rm c}/(1-\phi_{\rm c})$. The pressure is then

$$p = c_0 \int_{\zeta}^{\zeta^*} (1+e_{\rm bot})(\phi-\phi_{\rm c})^{1-m}\, d\zeta\,, \tag{32}$$

where the factor $(1+e_{\rm bot})\approx 1$ for $\phi_{\rm c}<0.05$. The integral over the porosity in eq. (32) can be quite accurately approximated, as shown in Appendix D. When the exponent in the specific surface function is $n=1$, the overpressure can be written as a function of temperature as

$$p \approx p_0\{\mathcal{G}((m-1)N_B F(T)) - \mathcal{G}((m-1)N_B F(T_0))\}\,. \tag{33}$$

The function $\mathcal{G}$ is defined as

$$\mathcal{G}(x) = \int_1^x \frac{1}{x}\exp(x)\, dx \tag{34}$$

and the pressure coefficient p_0 is

$$p_0 = \frac{(1+e_0)(\phi_0-\phi_{\rm c})\mu\omega T_{\rm f}}{(1-\phi_0)(\partial T/\partial\zeta)k_0 a}\,. \tag{35}$$

When the exponent in the specific surface function is different from 1, the solution for the pressure is

$$p \approx p_0 \int_{v_0}^{v} \frac{1}{x}(1+x)^{(m-1)/(n-1)}\, dx\,, \tag{36}$$

where the integration limits are $v=(n-1)N_B F(T)$ and $v_0=(n-1)N_B F(T_0)$. The pressure coefficient p_0 is given by expression (35), and it is the same for both cases of the exponent n in the specific surface function, $n=1$ and $n\neq 1$. The integral in eq. (36) can be expressed in closed form for integer exponents $(m-1)/(n-1)$.

It is seen from expression (32) that the pressure is limited above by a finite value when the exponent in the permeability function is $m<1$. However, if $m>1$, it is seen that the exponent in the solution (32) for pressure becomes negative, which leads to a rapid pressure build-up once the porosity approaches $\phi_{\rm c}$. This is also seen from Fig. 5, where the solution (32) is plotted for $m=2$, 3 and 4. This solution clearly shows how pressure increases rapidly when the sediments enter the thermal region where they become sealing, because the porosity is brought close to $\phi_{\rm c}$. The permeability coefficient in this case is $k_0=1\times10^{-18}$ m^2, and the burial rate is 50 m Myr^{-1}. (All other data are listed in Table 1.) The gravity number is $N_{\rm g}=7.5$, which is consistent with the moderate overpressures in the upper part of the basin.

The function $\mathcal{G}$ in the solution (eq. 33) takes as its argument the number $v(T)=(m-1)N_B F(T)$, which is a function of T. The function $v(T)$ is plotted in Fig. 6 for a typical value of N_B. It is seen that $v(T)$ is close to zero for T below the temperature window for cementation and ~ 1 in the window; it then increases rapidly for temperatures above the window. It is the large increase in the argument $v(T)$ of the function $\mathcal{G}$ that yields the large pressures for T above the temperature window where most of the porosity is lost.

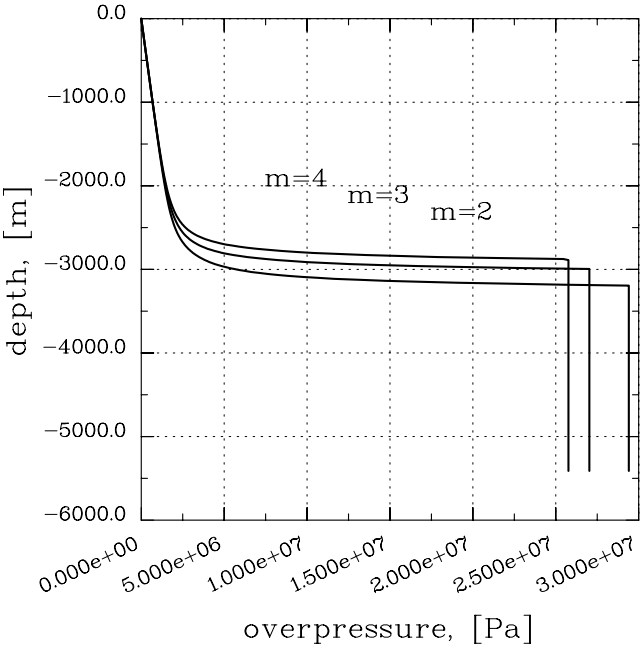

Figure 5. The pressure given by eq. (32) is plotted for permeability exponents $m=2$, 3 and 4. The other data are given in Table 1. The porosity in this case is given by a specific surface exponent $n=1$, which is plotted in Fig. 8. Note that the pressure build-up takes place when the porosity approaches the percolation threshold. The overpressure is plotted as a constant from the point where the fluid pressure becomes equal to the lithostatic pressure.

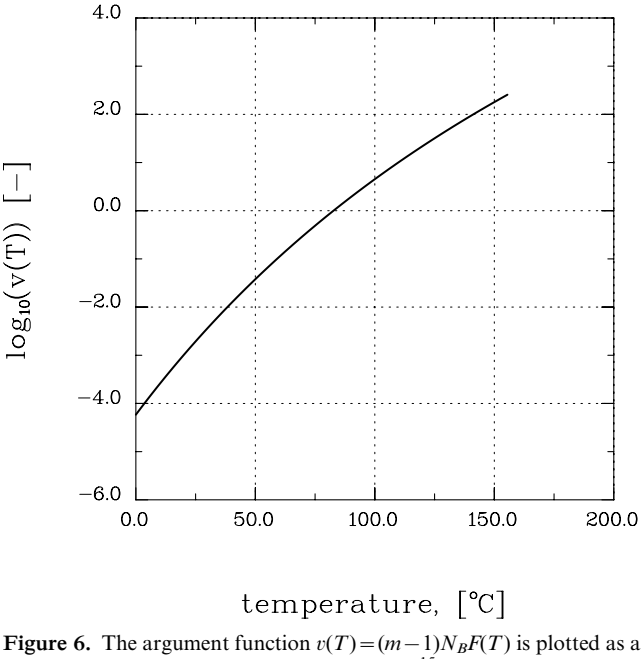

Figure 6. The argument function $v(T)=(m-1)N_B F(T)$ is plotted as a function T in °C for $m=2$ and $N_B=6.5\times10^{15}$, which are the values used in Fig. 5.

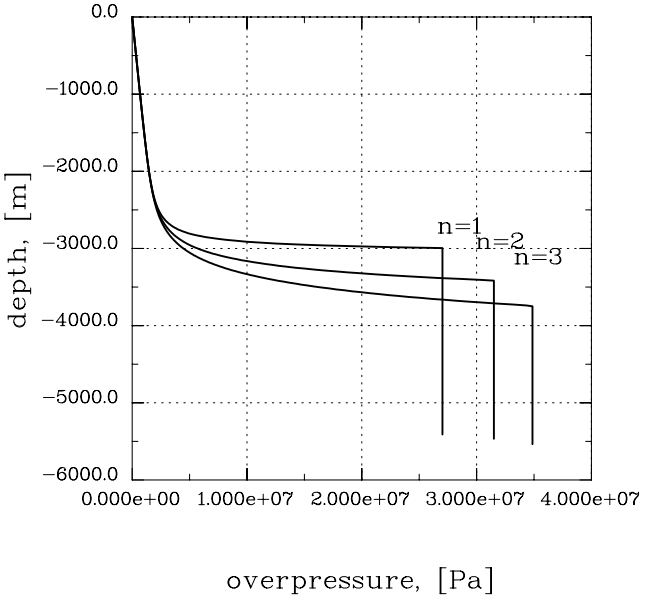

Figure 7. The pressure given by eq. (32) is plotted for specific surface exponents $n=1$, 2 and 3, when the permeability exponent is $m=3$. The other data are given in Table 1. The porosities for these three cases are plotted in Fig. 8.

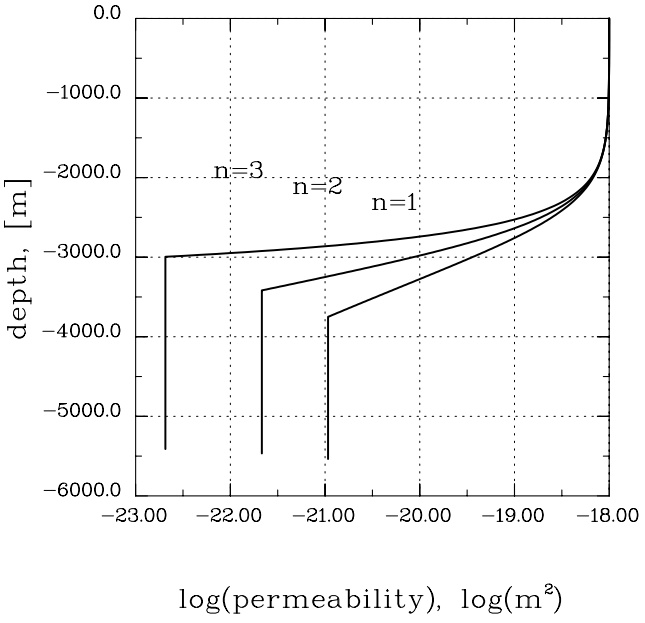

Figure 9. The permeabilities corresponding to the porosities in Fig. 8, when the permeability exponent is $m=3$ and the permeability coefficient is $k_0=1\times10^{-18}$ m^2.

The overpressure build-up for three different values of the exponent in the specific surface function, $n=1$, 2 and 3, is shown in Fig. 7. The porosities for these exponents are shown in Fig. 8. The large exponent, $n=3$, yields the smoothest decrease in porosity towards ϕ_c, and the overpressure build-up therefore takes place over a larger depth interval. The permeabilities corresponding to the porosities in Fig. 8 are shown in Fig. 9. The permeabilities in Fig. 9 decrease until the point where the fluid pressure reaches the lithostatic pressure, which is where hydrofracturing takes place. From this depth and further down the permeabilities are plotted as constants. It is seen from Fig. 9 that the permeability becomes as low as $1\times10^{-23}-1\times10^{-21}$ m^2 at the point where hydrofracturing takes place. This range of low permeabilities is compatible with observed permeabilities for shales (Neuzil 1994). The porosities are in the range 1–3 per cent above ϕ_c at the point where hydrofracturing occurs. The amount of fluid left to be expelled is therefore small.

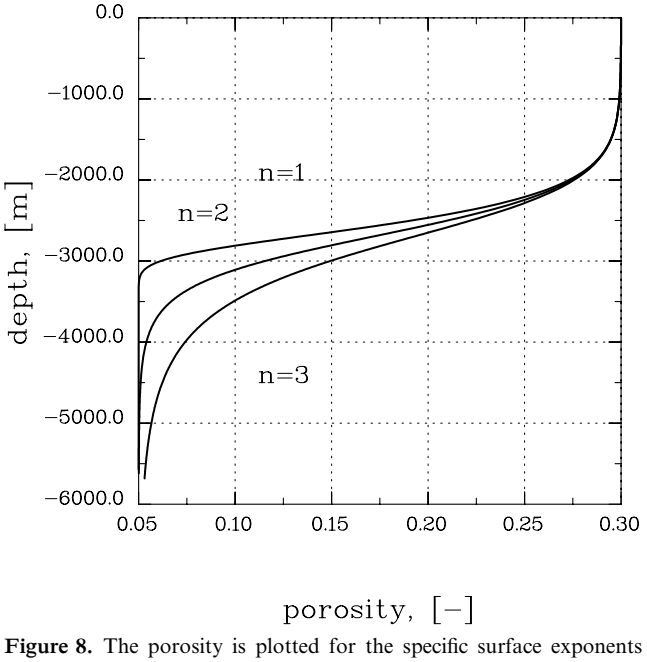

Figure 8. The porosity is plotted for the specific surface exponents $n=1$, 2 and 3. All the other data that enter the porosity calculations are taken from Table 1.

The heterogeneous nature of sediments implies that some sections of a sedimentary column will lose most of their porosity by cementation before other sections. The average vertical permeability over several sections will be dominated by the most sealing sections. Cementation therefore leads to pressure seals over beds that have preserved some of their porosity, where these sealed beds become overpressured. The importance of cementation as a pressure-generating mechanism is therefore partly due to the formation of seals, and not just the fact that fluid is expelled by the process. Note from Figs 5 and 8 that the pressure build-up takes place below the depth where less than half the porosity is left. The reduction in permeability is so strong that there is an overpressure build-up even though there is only a little fluid left to be expelled, when the porosity approaches ϕ_c.

Fig. 9 shows that the fluid pressure below the sealing depth interval are by no means limited by the lithostatic pressure. Pressure build-up caused by the expulsion of fluids from beds below seals must therefore be considered in association with hydraulic fracturing of the seals. The only way the fluid pressure can be limited by the lithostatic pressure (the overburden) is if the seals have their permeability enhanced in some way, when the fluid pressure approaches the lithostatic pressure. Hydrofracturing processes are not modelled here, although they are closely associated with the formation of low-permeability seals by cementation.

These results are similar to the results given in Wangen (1997), where an analytical solution for the overpressure was

given under the assumption of void ratio as an exponentially decreasing function of depth. Such a porosity–depth function was suggested by Athy (1930) and is still being used. The Athy behaviour of porosity as a function of depth makes sense when porosity is plotted as averages over thicker sequences. This is therefore the kind of average porosity that will naturally come out of numerical simulations. Although some sequences have lost their porosity due to cementation, others will have their porosities survive to larger depths. However, the computation of permeability from such average porosities should be performed with care, because the presence of even a thin cemented sheet will make a large difference in the vertical permeability of the formation.

8 CONCLUSIONS

The overpressure build-up caused by cementation of the pore space has been investigated. Particular attention was paid to the coupled processes of the expulsion of fluids caused by cementation and the reduction in permeability caused by the reduction in porosity.

It was shown that the overpressure decreases exponentially with time in a single layer at a constant depth when porosity reduction in the layer follows first-order kinetics. The half-life for the overpressure is the same as the half-life of the porosity reduction due to cementation. The initial overpressure is proportional to the initial porosity in the layer and the layer thickness and inversely proportional to the average permeability of the sediments above the layer as well as the time constant for the cementation process.

The overpressure build-up in a layer was then studied during constant burial along a constant thermal gradient. The sediment column above the layer was assumed to have the same average permeability regardless of its thickness during burial. The overpressure in the layer during burial was shown to increase with increasing rapidity of the kinetics, until a maximum was reached at roughly the same depth where half the porosity is lost due to cementation. From this depth and below, it was shown that the overpressure decreases rapidly, despite faster kinetics at higher temperatures during burial. This is because most of the porosity is lost, which implies that the potential for fluid expulsion is exhausted.

The fluid expulsion rates caused by the cementation of a single layer (or formation) can under optimal conditions reach or exceed the size of the expulsion rates of fluids expelled from all layers below. The optimal conditions for fluid expulsion take place right in the middle of the window for cementation.

Finally, the overpressure build-up in an entire sedimentary column was studied during burial. Cementation was allowed anywhere in the column, but it did not take place until a certain depth because kinetics are too slow in the upper part of the basin for cementation to be noticeable. The pressure build-up was studied for gravity numbers larger than 1, which implied that the upper part of the basin was low to moderately overpressured. This would have been the case for mechanical compaction in the upper part of the basin too, if it had been accounted for. It was shown that there is a steep increase in overpressure in the lower part of the window for cementation. The overpressure build-up would easily exceed the lithostatic pressure if it was not limited by the lithostatic pressure. This large increase in overpressure over a short depth interval was caused by both expulsion of fluid due to cementation and the strong reduction in permeability that takes place when the porosity approaches the percolation threshold at the lower end of the window for cementation. The overpressure below the point where the overpressure exceeds the lithostatic pressure is controlled by hydrofracturing, which enhances the permeability. The permeability reduction caused by cementation is so strong that the pressure build-up leads to hydrofracturing although there are only small amounts of fluid left to be expelled.

Cementation as the main cause for porosity reduction, when controlled by temperature, can therefore explain the pressure transition zones observed. Furthermore, the interval where the overpressure has its steepest rise towards the lithostatic pressure is shown to be slightly below the centre of the window for cementation.

ACKNOWLEDGMENTS

I would like to thank Per Arne Bjørkum and two anonymous referees for their comments on the manuscript.

REFERENCES

Aase, N.E, Bjørkum, P.A. & Nadeau, P., 1996. The effect of grain coating microquartz on preservation of reservoir porosity, *Am. Assoc. Petrol. Geol. Bull.,* **80,** 1654–1673.

Athy, L.F., 1930. Density, porosity, and compaction of sedimentary rocks, *Am. Assoc. Petrol. Geol. Bull.,* **14,** 1–24.

Audet, D.M. & Fowler, A.C., 1992. A mathematical model for compaction in sedimentary basins, *Geophys. J. Int.,* **110,** 577–590.

Bethke, M.C. & Corbet, T.F., 1988. Linear and nonlinear solutions for one-dimensional compaction flow in sedimentary basins, *Water Resource Res.,* **24,** 461–467.

Birchwood, R.A. & Turcotte, D.L., 1994. A unified approach to geopressuring, low-permeability zone formation, and secondary porosity generation in sedimentary basins, *J. geophys. Res.,* **99**(B10), 20 051–20 058.

Bjørkum, P.A., 1994. How important is pressure in causing dissolution of quartz in sandstones?, *Am. Assoc. Petrol. Geol. Ann. Mtng Program with Abstracts,* **3,** 105 (abstract).

Bjørkum, P.A., 1996. How important is pressure in causing dissolution of quartz in sandstones?, *J. sed. Res.,* **66,** 147–154.

Bjørkum, P.A. & Nadeau, P.H, 1996. A kinetically controlled fluid pressure and migration model, *Am. Assoc. Petrol. Geol. Ann. Mtng Program Abstracts,* San Diego, A15.

Bjørkum, P.A. & Nadeau, P.H, 1998. Temperature controlled porosity/permeability reduction, fluid migration, and petroleum exploration in sedimentary basins, *APPEA J.,* **38,** 453–464.

Bjørkum, P.A., Oelkers, E.H., Nadeau, P.H., Walderhaug, O. & Murphy, W.M., 1998. Porosity prediction in quartzose sandstones as a function of time, temperature, depth stylolite frequency, and hydrocarbon saturation, *Am. Assoc. Petrol. Geol. Bull.,* **82,** 637–648.

Bjørlykke, K., 1999. Principal aspects of compaction and fluid flow in mudstones, in *Muds and Mudstones: Physical and Fluid Flow Properties*, eds Aplin, A.C., Fleet, A.J. & Macquaker, J.H.S., *Geol. Soc. Lond. Spec. Publ.*, **158,** 73–78.

Bjørlykke, K., 1999. An overview of factors controlling rates of compaction, fluid generation and flow in sedimentary basins, in *Growth, Dissolution and Pattern Formation in Geosystems,* pp. 381–404, eds Jamtveit, B. & Meakin, P., Kluwer Academic, the Netherlands.

Bjørlykke, K. & Høeg, K., 1997. Effects on burial diagenesis on stress, compaction and fluid flow in sedimentary basins, *Mar. Petrol. Geol.,* **13,** 267–276.

Bredehoeft, J.D. & Hanshaw, B.B., 1968. On the maintenance of anomalous fluid pressures: I. Thick sedimentary sequences, *Geol. Soc. Am. Bull.,* **79,** 1097–1106.

Darby, D., Haszeldine, R.S. & Couples, G.D., 1996. Pressure cells and pressure seals in the UK central graben, *Mar. Petrol. Geol.,* **13,** 865–878.

Dewers, T. & Ortoleva, P.J., 1990. Interaction of reaction, mass transport, and rock deformation during diagenesis: mathematical modeling of intergranular pressure solution, stylolites, and differential compaction/cementation, in *Prediction of Reservoir Quality Through Chemical Modeling,* eds Meshri, I. & Ortholeva, P.J., *Am. Assoc. Petrol. Geol. Mem.*, **49,** 147–160.

Fowler, A.C. & Yang, X.-S., 1998. Fast and slow compaction in sedimentary basins, *SIAM J. appl. Math,* **59,** 365–385.

Fowler, A.C. & Yang, X.-S., 1999. Pressure solution and viscous compaction in sedimentary basins, *J. geophys. Res.,* **104**(B6), 12 989–12 997.

Gaarebstroom, L., Tromp, R.A.J., de Jong, M.C. & Brabdebburg, A.M., 1993. Overpressure in the Central North Sea: implications for trap integrity and drilling safety, in *Petroleum Geology of Northwest Europe: Proc. 4th Conf.,* pp. 1305–1313, ed. Parker, J.R., Geol. Soc. Lond., London.

Gibson, R.E., 1958. The progress of consolidation in a clay layer increasing in thickness with time, *Geotechnique,* **8,** 171–182.

Gorbachev, V.M., 1975. A solution of the exponential integral in the non-isothermal kinetics for linear heating, *J. Thermal Analysis,* **8,** 349–350.

Hermanrud, C., Wenaas, L., Teige, G.M.G., Vik, E., Bolaas, H.M.N. & Hansen, S., 1998. Shale porosities from well logs on Haltenbanken (offshore Mid-Norway) show no influence of overpressuring, *Am. Assoc. Petrol. Geol. Mem.,* **70,** 65–85.

Hunt, J.M., 1990. Generation and migration of petroleum from abnormally pressured fluid compartments, *Am. Assoc. Petrol. Geol. Bull.,* **74,** 1–12.

Lamée, C. & Guéguen, Y., 1996. Modeling of porosity loss during compaction and cementation of sandstones, *Geology,* **24,** 875–878.

Leonard, R.C., 1993. Distribution of sub-surface pressure in the Norwegian Central Graben and applications for exploration, *Petroleum Geology of Northwest Europe: Proc. 4th Conf.,* pp. 1295–1303, ed. Parker, J.R., Geol. Soc. Lond., London.

Lerche, I., 1990. *Basin Analysis. Quantitative Methods,* Vol. 1, Academic Press, New York.

Lichtner, P.C., 1985. Continuum model for simultaneous chemical reactions and mass transport in hydrothermal systems, *Geochim. Cosmochim. Acta,* **49,** 779–800.

Lichtner, P.C., 1988. The quasi stationary state approximation to coupled mass transport and fluid-rock interaction in a porous medium, *Geochim. Cosmochim. Acta,* **52,** 143–165.

Lou, X. & Vasseur, G., 1992. Contribution of compaction and aquathermal pressuring to geopressure and the influence of environmental conditions, *Am. Assoc. Petrol. Geol. Bull.,* **76,** 1550–1559.

Neuzil, C.E., 1994. How permeable are clays and shales?, *Water Resources Res.,* **30,** 145–150.

Oelkers, E.H., Bjørkum, P.A. & Murphy, W.M., 1992. The mechanism of porosity reduction, stylolite development and quartz cementation in North Sea sandstones, in *Water–Rock Interaction,* Vol. 2, pp. 1183–1186, eds Kharaka, Y.K. & Maest, A.S., Balkema, Rotterdam.

Oelkers, E.H., Bjørkum, P.A. & Murphy, W.M., 1993. Calculation of the rate and distribution of chemically driven quartz cementation on North Sea sandstones, in *Proc. 4th Int. Symp. Hydrothermal Reactions,* pp. 169–172, eds Cuney, M. & Cathelineau, M., Institut Lorain des Geosciences, Nancy, France.

Oelkers, E.H., Bjørkum, P.A. & Murphy, W.M., 1996. A petrographic and computational investigation of quartz cementation and porosity reduction in North Sea sandstones, *Am. J. Sci.,* **296,** 420–452.

Osborn, M.J. & Swarbrick, R.E., 1997. Mechanisms for generating overpressure in sedimentary basins: a reevaluation, *Am. Assoc. Petrol. Geol. Bull.,* **81,** 1023–1041.

Powley, D.E., 1990. Pressures and hydrogeology in petroleum basins, *Earth Sci. Rev.,* **29,** 215–226.

Sahimi, M., 1994. *Application of Percolation Theory,* Taylor & Francis, London.

Schneider, F., Potdevin, J.L, Wolf, S. & Faille, I., 1996. Mechanical and chemical compaction model for sedimentary basin simulators, *Tectonophysics,* **263,** 307–317.

Sharp, J.M., 1976. Momentum and energy balance equations for compacting sediments, *Math. Geol.,* **8,** 305–322.

Sharp, J.M. & Domenico, P.A., 1976. Energy transport in thick sequences of compacting sediment, *Geol. Soc. Am. Bull.,* **87,** 390–400.

Smith, J.E., 1971. Dynamics of shale compaction and evolution of pore-fluid pressure, *Math. Geol.,* **3,** 239–263.

Tester, J.W., Worley, G., Robinson, B.A., Grigsby, C.O. & Feerer, J.L., 1994. Correlating quartz dissolution kinetics in pure water from 25 to 625 °C, *Geochim. Cosmochim. Acta,* **58,** 2407–2420.

Ungerer, P., Burrus, J., Doligez, P.Y., Chénet, P.Y. & Bessis, F., 1990. Basin evaluation by integrated two-dimensional modeling of heat transfer, fluid flow, hydrocarbon generation and migration, *Am. Assoc. Petrol. Geol. Bull.,* **74,** 309–335.

Walderhaug, O., 1994. Temperatures of quartz cementation in Jurassic sandstones from the Norwegian continental shelf—evidence from fluid inclusions, *J. sed. Res.,* **A64,** 311–323.

Walderhaug, O., 1994. Precipitation rates for quartz cement in sandstones determined by fluid-inclusion microthermometry and temperature history modeling, *J. sed. Res.,* **A64,** 324–333.

Walderhaug, O., 1996. Kinetic modeling of quartz cementation and porosity loss in deeply buried sandstone reservoirs, *Am. Assoc. Petrol. Geol. Bull.,* **80,** 731–745.

Wangen, M., 1992. Pressure and temperature evolution in sedimentary basins, *Geophys. J. Int.,* **110,** 601–613.

Wangen, M., 1997. A simple model for overpressure build-up, *Geophys. J. Int.,* **130,** 757–764.

Wangen, M., 1998. Modeling porosity evolution and cementation of sandstones, *Mar. Petrol. Geol.,* **15,** 453–565.

Wangen, M., 1999. Modeling quartz cementation of quartzose sandstones, *Basin Res.,* **11,** 113–126.

Weast, R.C., (ed.), 1976. *The CRC Handbook of Chemistry and Physics,* CRC-Press, Cleveland, OH.

APPENDIX A: LITHOSTATIC PRESSURE

The lithostatic pressure, σ, at depth z is the pressure due to the total mass above z and can be written as

$$\sigma = \int_0^z ((1-\phi)\rho_s + \phi\rho_f) g \, dz \,, \tag{A1}$$

where the density of the sediment matrix and the density of fluid are ρ_s and ρ_f, respectively. The vertical position $z=0$ is the basin surface; there is no water above the basin surface. The fluid pressure is limited above by the lithostatic pressure. The overpressure, which is the fluid pressure minus the hydrostatic pressure, is therefore limited above by the lithostatic pressure minus the hydrostatic pressure. This pressure, denoted σ', becomes

$$\sigma' = \int_0^z (\rho_s - \rho_f)(1-\phi(z)) g \, dz \tag{A2}$$

and it is termed the excess lithostatic. Alternatively, the excess lithostatic pressure is conveniently expressed in the fully compacted coordinate, denote the ζ-coordinate, because $\Delta\zeta = (1-\phi)\Delta z$. The ζ-coordinate measures the height of a given z position down to the base of the sedimentary column as zero-porosity rock. The base of the sedimentary column becomes $\zeta = 0$. The ζ-coordinate is a constant for each grain deposited, and it is therefore a Lagrangian coordinate. The relation between

the ζ-coordinate and the z-coordinate is

$$z(\zeta)=\int_{\zeta}^{\zeta^*}\frac{d\zeta}{1-\phi(\zeta)}\,, \tag{A3}$$

where ζ^* is the height of the entire sedimentary column measured as porosity-free sediments from the base of the column. The excess lithostatic pressure (eq. A2) can then be written

$$\sigma'=(\rho_s-\rho_f)(\zeta^*-\zeta)g\,. \tag{A4}$$

The excess lithostatic pressure could also be expressed with real depth and an average porosity, $\bar{\phi}$, as

$$\sigma'=(\rho_s-\rho_f)(1-\bar{\phi})g\,z, \tag{A5}$$

where the average porosity down to the depth z is given as

$$\bar{\phi}=\frac{1}{z}\int_0^z\phi(z)\,dz\,. \tag{A6}$$

APPENDIX B: TEMPERATURE WHERE $\partial\phi/\partial T$ IS MAXIMUM

The rate of change of porosity $\partial\phi/\partial t$ reaches its maximum when $f(T)$ (eq. 21) reaches its maximum. It is convenient to replace T by the variable $x=T/T_f$ and then study $f(x)$. The exact expression for $f(x)$ is then

$$f(x)=\exp\left(-\frac{1}{x}-N_B\int_{x_0}^{x}\exp(-1/x)\,dx\right), \tag{B1}$$

where the integral in eq. (B1) is very well approximated by

$$\int_{x_0}^{x}\exp(-1/x)dx\approx F(x)-F(x_0)\,, \tag{B2}$$

as long as $x\ll 1$ (see Gorbachev 1975 for even better approximations). The function $F(x)$ is seen from eq. (9) to be $F(x)=x^2\exp(-1/x)$. The maximum of $f(x)$, given by the value x_{max}, solves $f'(x)=0$, which is equivalent to

$$x^2\exp(-1/x)=1/N_B\,. \tag{B3}$$

The value of $F(x_{max})$ is therefore seen to be $1/N_B$. Furthermore, $F(x_0)\ll F(x_{max})$ for x_0 given by the surface temperature, and the value $f(x_{max})$ can therefore be written as

$$f(x_{max})=\exp(-1/x_{max}-1)\,. \tag{B4}$$

It is seen from eq. (B3) that $1/x=\log(N_B)+2\log(x)$, which inserted into eq. (B4) yields

$$f(x_{max})=\frac{1}{\exp(1)N_B x_{max}^2}\,. \tag{B5}$$

The solution x_{max} of eq. (B3) is still needed to calculate $f(x_{max})$, which can be found by use of the approximation $2\log(x)-1/x\approx ax+b$, which leads to

$$x_{max}=-\frac{1}{a}\left(\log(N_B)+b\right) \tag{B6}$$

(see also Wangen 1999). The expression (22) is then obtained.

The temperature $T_{1/2}$, where half the porosity is lost, is seen from the porosity function (8) to be a solution of (in the case of first-order kinetics)

$$F(x_{1/2})=\frac{\log(2)}{N_B}\,, \tag{B7}$$

where $x_{1/2}=T_{1/2}/T_f$. $F(x_0)$ is, as above, negligible compared to $F(x_{1/2})$ for x_0 corresponding to the surface temperature. The temperature $T_{1/2}$ is seen to be close to T_{max}, because T_{max} is a solution of $F(x_{max})=1/N_B$, where N_B is a large number.

APPENDIX C: FLUID FLUXES DURING DEPOSITION

Conservation of fluid in a compacting sedimentary basin is conveniently expressed by the fully compacted vertical coordinate, denoted the ζ-coordinate, because it is a Lagrangian coordinate. A second reason for working with the ζ-coordinate is that fluid conservation is simply expressed as

$$\frac{\partial e}{\partial t}+\frac{\partial v}{\partial\zeta}=0\,, \tag{C1}$$

where e is the void ratio and v is the Darcy velocity. The fluid density is assumed constant. The Darcy velocity at a point ζ is then obtained from eq. (C1) by integration,

$$v(\zeta,t)=-\int_0^{\zeta}\left(\frac{\partial e}{\partial t}\right)_{\zeta}d\zeta\,. \tag{C2}$$

The integral is trivial to carry out when the void ratio is given as a function of the depth from the surface measured as a ζ-depth, and when the burial rate ω is constant along the ζ-axis. The top of the basin along the ζ-axis is $\zeta^*=\omega t$, and the void ratio as a function of the ζ-depth measured from the top is

$$e=e(\omega t-\zeta)\,. \tag{C3}$$

Note that the void ratio is a function of one single argument, the ζ-depth $\omega t-\zeta$. The integral (C2) becomes

$$v(\zeta,t)=\omega(e(\zeta,t)-e(0,t))=\omega(e-e_{bot})\,. \tag{C4}$$

The integration (C2) can be carried out in the same way when the void ratio is a function of the temperature during burial along a constant thermal gradient. The porosity function (8) is an example of porosity (void ratio) as a function of temperature during burial. The integral can then be written (see eq. D2 for the change of integration variable from ζ to T)

$$v=-\int_0^{\zeta}\left(\frac{\partial e}{\partial t}\right)_{\zeta}d\zeta=-\int_0^{\zeta}\frac{\partial e}{\partial T}\frac{\partial T}{\partial t}\,d\zeta=\omega\int_{T_{bot}}^{T}\frac{\partial e}{\partial T}\,dT$$

$$=\omega(e-e_{bot})\,. \tag{C5}$$

The fluid flux at any point in a sedimentary column caused by cementation controlled by temperature is simply proportional to the burial rate and the difference between the void ratio at the given depth and the void ratio at the base of the column.

APPENDIX D: INTEGRATION OF $(\phi-\phi_c)^p$ ALONG THE ζ-AXIS

The integral of $(\phi-\phi_c)^p$ along the ζ-axis can be written

$$\int_{\zeta}^{\zeta^*}(\phi-\phi_c)^p\,d\zeta=(\phi_0-\phi_c)^p\int_{\zeta}^{\zeta^*}\exp(-pN_B(F(T)-F(T_0)))\,d\zeta \tag{D1}$$

when the exponent in the specific surface function is $n=1$. Integration in ζ can be replaced with integration in temperature by

$$d\zeta = -\frac{1}{\partial T/\partial \zeta}\, dT\,, \tag{D2}$$

because $T=(\partial T/\partial\zeta)(\zeta^*-\zeta)+T_0$. Furthermore, the integration in temperature can be replaced by an integration over $v(T)=pN_BF(T)$. It is shown in Appendix B that $F(T)\approx\exp(a(T/T_f)+b)$, which leads to

$$dT \approx \frac{T_f}{av}\, dv\,. \tag{D3}$$

The integration (D1) can then be written, after a change of variable to v,

$$\int_{\zeta}^{\zeta^*} (\phi-\phi_c)^p\, d\zeta = \frac{(\phi_0-\phi_c)^p T_f}{(\partial T/\partial\zeta)a} \exp(-v(T_0)) \int_{v(T_0)}^{v(T)} \frac{\exp(v)}{v}\, dv\,. \tag{D4}$$

The factor $\exp(-v(T_0))\approx 1$ for $T_0=0^\circ$C and it can be left out, which then yields the solution (33). The same change of integration variable leads to the expression (36) for the overpressure in the case of $n\neq 1$.